Robust Tracking Control for a Piezoelectric Actuator[1]

M. Salah†, M. McIntyre*, D. Dawson†, and J. Wagner‡

†Departments of Electrical and Computer Engineering, Clemson University, Clemson, SC 29634

‡Departments of Mechanical Engineering, Clemson University, Clemson, SC 29634

*Adjunct Faculty with the Department of Electrical and Computer Engineering at the University of Louisville, Louisville Ky 40292

E-mail: msalah@ces.clemson.edu

Abstract: In this paper, a hysteresis model-based nonlinear robust controller is developed for a piezoelectric actuator, utilizing a Lyapunov-based stability analysis, which ensures that a desired displacement trajectory is accurately tracked.

1 Introduction

Piezoelectric actuator (PZTA) based systems are emerging as an important technology for precise positioning and have received wide attention in both the scientific and industrial communities. These devices are capable of completing high precision actuation tasks. They are often utilized in motion actuation applications, due to their high stiffness, fast response, and physically unlimited resolution [17], and can be used as either sensors or actuators in control systems. The advantages of the PZTA [13] include: 1) no wear, 2) high efficiency, 3) almost infinite small positioning ability, 4) ultra fast expansion, and 5) capability to deliver large actuation forces. These micro-positioning elements play a big role in many vital applications such as scanning tunneling microscopy [30], scanning probe microscopy ([9] and [22]), laser applications [28], and hydraulic servo control systems [5].

Despite the advantages of PZTA's for micro positioning applications, the actuator's positioning response shows a strong hysterical activity due to their composition from ferroelectric ceramic materials. Specifically, an applied voltage is typically the input control signal which activates the PZTA. In the event that the input control voltage is relatively large, the PZTA exhibits a significant amount of distortion due to the inherent hysteresis in the device, and this effect may reduce the stability of the system in feedback control applications [25]. Due to this nonlinear behavior, one would expect difficulties in using PZTA's for precise tracking control applications. Hence, nonlinear control strategies are needed for the use of the PZTA's in micro positioning and tracking systems.

Past PZTA research has focused on establishing an accurate dynamic actuator model ([3], [16], and [29]), while other research has focused on the development of active control strategies for use in precise positioning and tracking applications ([12], [13], [17], [24], and [26]). In [11], the authors provided a concise literature summery with regard to modeling the PZTA's dynamics. Recently, the literature has focused on the development of alternate models to describe the hysteresis within the PZTA, due to the challenging nonlinear nature of this phenomenon. In [29], the authors included a nonlinear spring element into the hysteresis model and utilized a Maxwell-slip structure, while the authors of [14] used a support vector regression nonlinear model and neural networks. The authors of [15] and [20] found that voltage to displacement linearization of a PZTA may be achieved if the control input is the applied electric charge rather than the applied voltage. Furutani *et al.* [10] was able to improve the PZTA control strategy by combining induced charge feedback with inverse transfer function compensation. Vautier and Moheimani [25] showed that applying an electric charge to control the position reduces the effects of the nonlinearity in the PZTA dynamics. They also showed experimental results demonstrating the effectiveness of using electrical charge. Further, Main *et al.* [19] presented experimental data from tests for both voltage and charge control which showed that charge control is significantly more linear and less hysteretic than voltage control over the same actuator displacement range.

In [18], the authors proposed a new mathematical model to describe complex hysteresis that is based on a new parameter called turning voltage of a PZTA. In their work, the authors of [18] were able to utilize this parameter to suppress the inherent hysteresis to within $\pm 1\%$ full span range of a PZTA. Shieh *et al.* in [23] developed a parametrized hysteretic friction function, based on the LuGre model, to describe the PZTA hysteresis behavior. Thus, these researchers were able to design an adaptive displacement tracking control with a parameter adaptation algorithm. In [3], Bashash and

[1]This research was supported in part by a DOC Grant, an ARO Automotive Center Grant, a DOE Contract, a Honda Corporation Grant, and a DARPA Contract.

Jalili presented a perturbation estimation technique to compensate for the structural nonlinearities and unmodeled PZTA dynamics. In their work, the authors of [3] validated the proposed model by experimental tests using a PZTA-driven nano-stager with capacitive position sensor.

Other research in the literature has focused on the development of intelligent control schemes for the precise control of PZTA's. Some of these designs were based on the inverse hysteresis model that is assumed to be known *a priori*, so feedforward techniques can be utilized in the control design ([2] and [16]). Others, such as [4], [6], [12] and [13], applied a feedback linearization to compensate for the hysteresis dynamics and then a tracking controller was implemented. Wu and Zou in [27] presented an inversion-based iterative control approach to compensate for both the hysteresis and the vibrational dynamics variations during high-speed, and large range tracking. Neural networks and fuzzy controls were also utilized to model the PZTA hysteresis nonlinearities and control the micro motion of the PZTA ([13] and [26]). In [17], the authors proposed a robust control strategy for precise positioning tracking. The implementation of their control law requires only a knowledge of the estimated system parameters and their corresponding bounds as well as the bound of the hysteresis effect including disturbances. In [24], Stepanenko and Su introduced and implemented an approximation function to compensate for the hysteresis nonlinearities by fuzzy logic techniques.

In this paper, the displacement of a PZTA is actively controlled to track a desired trajectory. A nonlinear robust control strategy is developed based on the feedback of the PZTA charge, and partial knowledge of the hysteresis model. Charge steering approach eliminates the effect of the hysteresis in the PZTA and provides better robust control over the voltage steering approach [1]. The charge measurement is obtained by measuring the voltage across a capacitor that is added in-series to the PZTA circuit. A Lyapunov-based analysis, which proves precise tracking, is utilized to develop the control strategy. This paper is organized as follows. In Section 2, a Coleman-Hodgdon-based hysteresis model along with the piezoelectric actuator dynamics are presented as well as the required assumptions for the system. In Section 3, a nonlinear robust control scheme is developed along with the stability analysis which verifies that the piezoelectric desired displacement can be tracked. Finally, concluding remarks are provided in Section 4.

2 PZTA System Model

2.1 PZTA Elongation Dynamics

A PZTA with a single elongation axis, depicted in Figure 1, can be dynamically modeled as

$$m\ddot{y} + F_L = F_p \tag{1}$$

where $m \in \mathbb{R}$ denotes the PZTA mass, $L \in \mathbb{R}$ denotes the non-activated length of the PZTA, $F_p(t) \in \mathbb{R}$ denotes the force generated by the PZTA elongation, $F_L(y, \dot{y}) \in \mathbb{R}$ denotes the perpendicular forces acting on the PZTA, $y(t), \dot{y}(t), \ddot{y}(t) \in \mathbb{R}$ are the displacement, velocity, and acceleration, respectively, of the PZTA effective tip of elongation. An equivalent circuit model of the PZTA can be described as shown in Figure 2.

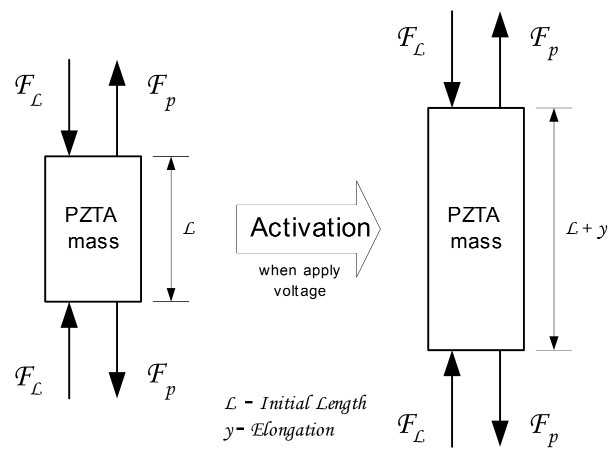

Figure 1: PZTA elongation induced by applied voltage

In this schematic, $V(t) \in \mathbb{R}$ denotes the applied input control voltage, $\dot{q}(t) \in \mathbb{R}$ represents the current flowing through the PZTA, since $i(t) = \dot{q}(t)$. Further, $C_m \in \mathbb{R}^+$ is a series connected capacitor that facilitates the measurement of $q(t) \in \mathbb{R}$, through a measurement of the voltage $V_m(t) \in \mathbb{R}$ across C_m, recall that $q = C_m V_m$. In Figure 2, the circuit element indicated by H models the inherent hysteresis between the voltage $V_h(t) \in \mathbb{R}$ and the induced charge $q(t)$. A subsequent section will further define the hysteresis model. The parameter $C_c \in \mathbb{R}^+$ is the internal capacitance of the PZTA, $\dot{q}_c(t) \in \mathbb{R}$ is the current flowing through C_c, and $V_c(t) \in \mathbb{R}$ is the voltage across this capacitance. Finally, the circuit element indicated by T_{em} represents the subsequently defined elongation model, where $T_{em} \in \mathbb{R}^+$ is the elongation constant [17], and $\dot{q}_p(t) \in \mathbb{R}$ denotes the current flowing through this circuit branch.

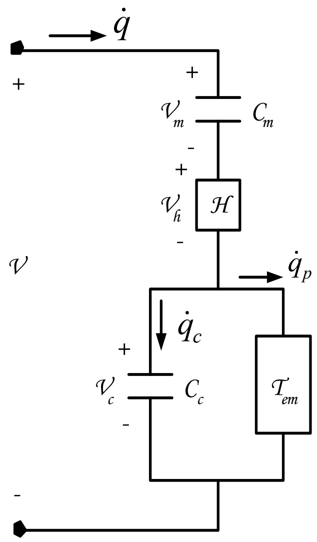

Figure 2: PZTA equivalent circuit model

2.2 Hysteresis Model

A nonlinear hysteresis model $H(V_h) \in \mathbb{R}$ can be defined to describe the relationship between the input voltage $V_h(t)$ and the induced charge $q(t)$. For this paper, a Duhem-based hysteresis model can be defined as [8]

$$q = H(V_h) \triangleq f(V_h) + d(V_h) \tag{2}$$

where $f(V_h) \in \mathbb{R}$ is a subsequently defined signal. The variable $d(V_h) \in \mathbb{R}$ is defined as

$$d \triangleq \begin{cases} d_{inc}, & \text{if } \dot{V}_h(t) > 0, \text{ and } V_h(t) > V_{h_o} \\ d_{dec}, & \text{if } \dot{V}_h(t) < 0, \text{ and } V_h(t) < V_{h_o} \end{cases} \tag{3}$$

where

$$d_{inc} \triangleq [q_o - f(V_{h_o})] e^{-\delta(V_h - V_{h_o})} + e^{-\delta V_h} \int_{V_{h_o}}^{V_h} \left(g(\tau) - f'(\tau) \right) e^{\delta\tau} d\tau \tag{4}$$

$$d_{dec} \triangleq [q_o - f(V_{h_o})] e^{-\delta(V_{h_o} - V_h)} + e^{\delta V_h} \int_{V_{h_o}}^{V_h} \left(g(\tau) - f'(\tau) \right) e^{-\delta\tau} d\tau \tag{5}$$

where $q_o \in \mathbb{R}$ is the induced charge at $t = t_o$, $V_{h_o} \in \mathbb{R}$ is the input voltage at $t = t_o$, $\delta \in \mathbb{R}^+$ is a constant, and $f'(\tau) \in \mathbb{R}$ is the partial derivative of $f(V_h)$ with respect to the input voltage $V_h(t)$. The signals $d(V_h), f(V_h)$, and $g(V_h) \in \mathbb{R}$ have the following properties [7]:

Property 1: The function $f(V_h)$ is piecewise smooth, monotone increasing, and odd.

Property 2: The function $g(V_h)$ is piecewise continuous, and even.

Property 3: The function $f(V_h)$ is known, and invertible, such that $\overline{V}_h = f(V_h)$, and $V_h = f^{-1}(\overline{V}_h)$.

Property 4: The partial derivative of $f(V_h)$ with respect to $V_h(t)$ (*i.e.*, $\frac{\partial f(V_h)}{\partial V_h}$) is not identically zero, hence, $f'(\infty) = \eta_o$, where $\eta_o \in \mathbb{R}^+$ is a constant.

Property 5: The function $g(V_h)$ has a finite upper limit $\left(i.e., f'(\infty) = g(\infty)\right)$ where $f'(V_h) \geq g(V_h)$.

Property 6: The function $d(V_h)$ is bounded as

$$|d| \leq \eta_d \tag{6}$$

where $\eta_d \in \mathbb{R}^+$ is a constant (see Appendix A in [21] for proof).

2.3 Elongation Model

Two linear relationships model the elongation action of the PZTA. One relationship models the effect of the induced charge $q_p(t)$ on the displacement of the elongation axis, $y(t)$, and can be written as [17]

$$q_p \triangleq T_{em} y. \tag{7}$$

The second relationship depicts the force $F_p(t)$ imparted by the elongation action as a function of the voltage $V_c(t)$ which becomes [17]

$$F_p \triangleq T_{em} V_c. \tag{8}$$

In (7) and (8), T_{em} is the elongation constant inherent to the PZTA.

2.4 Dynamic Model and Assumptions

To facilitate the subsequent control objective, a dynamic expression is desired that relates the displacement of the elongation axis $y(t)$ as a function of charge $q(t)$ induced within the PZTA. The advantage of working with such a dynamic model is clear due to the lack of the hysteresis terms which has been discussed in the literature (see [10], [19], and [25]). From Figure 2, it is clear that the induced charge $q(t)$ can be described as

$$q = C_c V_c + q_p. \tag{9}$$

From (9), the expression in (1) can be written as

$$m\ddot{y} + \overline{F}_L = \left(\frac{T_{em}}{C_c} \right) q \tag{10}$$

where (7) and (8) were utilized. The variable $\overline{F}_L(y,\dot{y}) \in \mathbb{R}$ is defined as

$$\overline{F}_L \triangleq F_L + \left(\frac{T_{em}^2}{C_c}\right) y. \tag{11}$$

To facilitate the tracking control design, three assumptions frame the analysis.

Assumption 1: The PZTA's parameters m, C_c, C_m, and T_{em} are assumed to be known, and constants with respect to time.

Assumption 2: The displacement $y(t)$, and velocity $\dot{y}(t)$ of the PZTA effective tip are assumed to be measurable.

Assumption 3: It is assumed that the forces $F_L(y,\dot{y})$ and their first time derivative $\dot{F}_L(y,\dot{y},\ddot{y})$ are bounded $\left(i.e., F_L(y,\dot{y}), \dot{F}_L(y,\dot{y},\ddot{y}) \in L_\infty\right)$ provided $y(t)$, $\dot{y}(t), \ddot{y}(t) \in L_\infty$.

3 Robust Control Development

3.1 Control Design Objective

The control objective is to ensure that the displacement $y(t)$ of the PZTA effective tip tracks the desired trajectory $y_d(t) \in \mathbb{R}$ in the following sense

$$|y_d(t) - y(t)| \leq \varepsilon \quad \text{as} \quad t \to \infty \tag{12}$$

where $\varepsilon \in \mathbb{R}^+$ is a constant that can be selected arbitrary small.

Assumption 4: The subsequent analysis requires that a desired trajectory is selected such that $y_d(t)$, $\dot{y}_d(t)$, and $\ddot{y}_d(t)$ are bounded (*i.e.*, $y_d(t), \dot{y}_d(t), \ddot{y}_d(t) \in L_\infty$) where $\dot{y}_d(t), \ddot{y}_d(t) \in \mathbb{R}$.

To facilitate the subsequent development, a filtered tracking error signal, denoted by $r(t) \in \mathbb{R}$, is defined as

$$r \triangleq \dot{e} + \alpha e \tag{13}$$

where $\alpha \in \mathbb{R}^+$ is a control gain. The variable $e(t) \in \mathbb{R}$ is defined as

$$e \triangleq y_d - y. \tag{14}$$

Based on the definition of $e(t)$ in (14), it is clear that if $|e(t)| \leq \varepsilon$ as $t \to \infty$, then $|y_d(t) - y(t)| \leq \varepsilon$ as $t \to \infty$, thus, meeting the control objective.

3.2 Closed-Loop Error System

To facilitate the development of a closed-loop error system, a control strategy must be developed to account for the inherent hysteresis that exists between the input voltage $V_h(t)$ and the induced charge $q(t)$. To continue this development, the charge as defined in (2) can be rewritten as

$$q = f(V - V_m - V_c) + d(V_h). \tag{15}$$

It is clear from Figure 2 that an expression for $V_h(t)$ can be stated as

$$V_h = V - V_m - V_c. \tag{16}$$

To meet the previously stated control objective, the control input $V(t)$ as shown in Figure 2 can be designed as

$$V \triangleq V_m + V_c + f^{-1}\left(\overline{V}_h\right) \tag{17}$$

where $\overline{V}_h(t) \in \mathbb{R}$ is a subsequently designed auxiliary control signal, and Property 3 was utilized.

Remark 1 *From (9), the voltage $V_c(t)$ can be obtained as*

$$V_c = \frac{1}{C_c}(q - q_p) \tag{18}$$

where the charge $q_p(t)$ is computed from (7), and the charge $q(t)$ is computed from the measurement of $V_m(t)$ across the capacitor C_m (i.e., $q = C_m V_m$).

Utilizing (17), the hysteresis between the voltage and change in (15) can be written as

$$q = H(V_h) \triangleq \overline{V}_h + d(V_h). \tag{19}$$

To continue the closed-loop error system development, an auxiliary error signal $s(t) \in \mathbb{R}$ is defined as

$$s \triangleq q_d - q \tag{20}$$

where $q_d(y,\dot{y}) \in \mathbb{R}$ is a subsequently designed auxiliary signal. From (19), the auxiliary signal $s(t)$ can be rewritten as

$$s = q_d - \overline{V}_h - d(V_h). \tag{21}$$

The auxiliary control signal $\overline{V}_h(t)$ is designed as

$$\overline{V}_h \triangleq q_d + k_s s \tag{22}$$

where $k_s \in \mathbb{R}^+$ is a constant.

Remark 2 *The expression in (22) can be expanded as*

$$\overline{V}_h \triangleq q_d + k_s(q_d - q) \tag{23}$$

where (20) is utilized, and the charge $q(t)$ is computed from the measurement of $V_m(t)$ across the capacitor C_m (i.e., $q = C_m V_m$).

From (22), the expression in (21) can be simplified as

$$s = -k_s s - d\left(V_h\right). \tag{24}$$

The auxiliary error signal $s\left(t\right)$ can be upper bounded as

$$s \leq \frac{|d|}{1+k_s} \leq \eta_s \tag{25}$$

where $\eta_s \in \mathbb{R}^+$ is a constant and Property 6 was utilized.

With the control concept in place to account for the voltage to charge hysteresis, the dynamic model as defined in (10) is now incorporated to complete the closed-loop error system development. From the PZTA dynamics, described in (10), the following expression can be obtained

$$m\ddot{y} + \overline{F}_L + \left(\frac{T_{em}}{C_c}\right)s = \left(\frac{T_{em}}{C_c}\right)q_d \tag{26}$$

where (20) was utilized. To facilitate the development of the closed-loop error system for $r(t)$, the first time derivative of (13) is taken and then both sides are multiplied by m, thus, obtaining the following expression

$$m\dot{r} = m\ddot{y}_d + \overline{F}_L + \left(\frac{T_{em}}{C_c}\right)s - \left(\frac{T_{em}}{C_c}\right)q_d + \alpha m\dot{e} \tag{27}$$

where (26), and the first time derivative of (14) were utilized. To facilitate the subsequent analysis, the expression in (27) is rewritten as

$$m\dot{r} = \widetilde{N} + N_d - e + \left(\frac{T_{em}}{C_c}\right)s - \left(\frac{T_{em}}{C_c}\right)q_d \tag{28}$$

where the auxiliary signal $\widetilde{N}\left(y,\dot{y}\right) \in \mathbb{R}$ is defined as

$$\widetilde{N} \triangleq N - N_d. \tag{29}$$

The variable $N(y,\dot{y},\ddot{y}_d) \in \mathbb{R}$ is defined as

$$N \triangleq m\ddot{y}_d + \overline{F}_L + e + \alpha m\dot{e} \tag{30}$$

and the variable $N_d(t) \in \mathbb{R}$ is defined as

$$\begin{aligned} N_d &\triangleq N|_{y=y_d,\dot{y}=\dot{y}_d} \\ &= m\ddot{y}_d + \overline{F}_{Ld} \end{aligned} \tag{31}$$

where $\overline{F}_{Ld}\left(y_d,\dot{y}_d\right) \in \mathbb{R}$, introduced in (11), is evaluated at $y_d\left(t\right)$ and $\dot{y}_d\left(t\right)$. Based on (28), the signal $q_d\left(y,\dot{y}\right)$ is designed as

$$q_d = \left(\frac{C_c}{T_{em}}\right)\left[k_r r + \frac{1}{\varepsilon}\rho\left(\|z\|\right)^2\|z\|^2 r\right] \tag{32}$$

where $k_r \in \mathbb{R}^+$ is a constant control gain, $\varepsilon \in \mathbb{R}^+$ is a small constant, and $\rho\left(\|z\|\right) \in \mathbb{R}$ is a function of norm $z\left(t\right) \in \mathbb{R}^2$. The variable $z\left(t\right)$ is defined as

$$z = \left[\begin{array}{cc} e & r \end{array}\right]^T \tag{33}$$

where $r\left(t\right)$ and $e\left(t\right)$ were introduced in (13) and (14), respectively. By utilizing (29) through (31), the following inequality can be developed (see Appendix C in [21] for further details)

$$\left|\tilde{N}\right| \leq \rho\left(\|z\|\right)\|z\|. \tag{34}$$

After substituting (32) into (28), the following closed-loop error system can be obtained

$$\begin{aligned} m\dot{r} &= \widetilde{N} + N_d - e + \left(\frac{T_{em}}{C_c}\right)s - k_r r \\ &\quad -\frac{1}{\varepsilon}\rho\left(\|z\|\right)^2\|z\|^2 r. \end{aligned} \tag{35}$$

3.3 Stability Analysis

Theorem 1 *The controller given in (17), (22), and (32) ensures that $|e(t)| \leq \varepsilon$ as $t \to \infty$ provided the control gain k_r, introduced in (32), is sufficiently large, hence, $e\left(t\right)$ is practically regulated to zero. A secondary objective is that all closed-loop signals are also bounded*

Proof: See Appendix B in [21].

4 Conclusion

This work develops a nonlinear robust controller for a piezoelectric actuator where its effective tip is driven to track a desired trajectory. The PZTA charge feedback along with the partial knowledge of the hysteresis model is utilized to design a nonlinear robust control strategy.

References

[1] H. Adriaens, W. De-Koning, and R. Banning, "Modeling Piezoelectric Actuators," *IEEE/ASME Trans. on Mechatronics*, Vol. 5, No. 4, pp. 331-341, (2000)

[2] H. Ahn, "Design of a Repetitive Control System for a Piezoelectric Actuator Based on the Inverse Hysteresis Model," *Proc. 4th International Conference on Control and Automation*, Montreal, Canada, June 2003, pp. 128-132.

[3] S. Bashash, and N. Jalili, "Real-Time Identification of Piezoelectric Actuator Nonlinearities with Application to Precision Trajectory Control," *Proc. American Control Conference*, Minneapolis, MN, June 2006, pp. 3308-3313.

[4] B. Chen, T. Lee, C. Hang, Y. Guo, and S. Weerasooriya, "An H_∞ Almost Disturbance Decoupling Robust Controller Design for a Piezoelectric Bimorph Actuator with Hysteresis," *IEEE Trans. on Control, Systems Technology*, Vol. 7, No. 2, pp. 160-174, (1999).

[5] M. Chiang, L. Lee, and K. Huang, "Development of a Hydraulic-Piezoelectric-Actuator for Hybrid Positioning Control

with Large Stroke, High Loading and Sub-Micrometer Accuracy," *Proc. IEEE International Conference on Mechatronics*, Taipei, Taiwan, July 2005, pp. 45-49.

[6] G. Choi, H. Kim, and G. Choi, "A study on Position Control of Piezoelectric Actuators," *Proc. IEEE International Symposium on Industrial Electronics*, Vol. 3, pp. 851 - 855, (1997).

[7] B. Coleman, and M. Hodgdon, "A constitutive relation for rate-independent hysteresis in ferromagnetically soft materials," *International Journal of Engineering Science*, Vol. 24, No. 6, pp. 897-919, (1986).

[8] B. Coleman, and M. Hodgdon, "On a class of constitutive relations for ferromagnetic hysteresis," *Archive for Rational Mechanics and Analysis*, Vol. 99, No. 4, pp. 375-396, (1987), DOI 10.1007/BF00282052, URL http://dx.doi.org/10.1007/BF00282052.

[9] A. Daniele, S. Salapaka, M. Salapaka, and M. Dahleh, "Piezoelectric Scanners for Atomic Force Microscopes: Design of Lateral Sensors, Identification and Control," *Proc. American Control Conference*, San Diego, CA, June 1999, pp. 253-257.

[10] K. Furutani, M. Urushibata, and N. Mohri, "Displacement Control of Piezoelectric Element by Feedback of Induced Charge," *Journal of Nanotechnology*, pp. 93-98, (1998).

[11] Y. Huang, and D. Lin, "Tracking Control of a Piezoelectric Actuator based on Experiment Hysteretic Modeling," *Proc. IEEE/ASME International Conference on Advanced Intelligent Mechatronics*, July 2003, Vol. 1, pp. 301-313.

[12] C. Hwang, Y. Chen, and C. Jan, "Trajectory Tracking of Large-Displacement Piezoelectric Actuators using Nonlinear Observer-based Variable Structure Control," *IEEE Trans. on Control, Systems Technology*, Vol. 13, No. 1, pp. 56-66, (2005).

[13] C. Hwang, and C. Jan, "State Estimator-based Feedback Control for a Class of Piezoelectric Systems with Hysteresis Nonlinearity," *IEEE Trans. on System, Man, and Cybernetics - Part A: Systems and Humans*, Vol. 35, No. 5, pp. 654-664, (2005).

[14] H. Ji, S. Yang, Z. Wu, and G. Yan, "Precision Control of Piezoelectric Actuator using Support Vector Regression Nonlinear Model and Neural Networks," *Proc. 4th IEEE International Conference on Machine Learning and Cybernetics*, Guangzhou, China, Aug 2005, Vol. 2, pp. 1186-1191.

[15] H. Kaizuka, and B. Sui, "A Simple Way to Reduce Hysteresis and Creep when using Piezoelectric Actuators," *Japanese Journal of Applied Physics*, Vol. 27, No. 5, pp. L773-L776, (1988).

[16] B. Lee, S. Yang, and K. Ahn, "Precision Control of Piezoelectric Actuator using Inverse Hysteresis Model and Neuro Control," *Proc. 7th IEEE Korea-Russia International Symposium on Science and Technology*, Uni. of Ulsan, Republic of Korea, July 2003, Vol. 1, pp. 273-238.

[17] H. Liaw, D. Oetomo, B. Shirinzadeh, and G. Alici, "Robust Motion Tracking Control of Piezoelectric Actuation Systems," *Proc. IEEE International Conference on Robotics and Automation*, Orlando, FL, May 2006, pp. 1414-1419.

[18] S. Lining, R. Changhai, R. Weibin, and C. Liguo, "Tracking Control of Piezoelectric Actuator Based on a New Mathematical Model," *Journal of Micromechanics and Microengineering*, Vol. 14, pp. 1439-1444, (2004).

[19] J. Main, E. Garcia, and D. Newton, "Precision Position Control of Piezoelectric Actuators using Charge Feedback ," *Journal of Guidance, Control, and Dynamics*, Vol. 18, No. 5, pp. 1068-1073, (1995).

[20] C. Newcomb, and I. Flinn, "Improving the linearity of Piezoelectric ceramic actuators," *Electronic Letters*, Vol. 18, No. 11, pp. 442-444, (1982).

[21] M. Salah, M. McIntyre, D. Dawson, and J. Wagner, "Robust Tracking Control for a Piezoelectric Actuator," Clemson University CRB Technical Report, CU/CRB/9/14/06/#1, http://www.ces.clemson.edu/ece/crb/publictn/tr.htm.

[22] G. Schitter, and A. Stemmer, "Identification and Open-Loop Tracking Control of a Piezoelectric Tube Scanner for High Speed Scanning-Probe Microscopy," *IEEE Trans. on Control, Systems Technology*, Vol. 12, No. 3, pp. 449-454, (2004).

[23] H. Shieh, F. Lin, P. Huang, and L. Teng, "Adaptive Displacement Control with Hysteresis Modeling for Piezoactuated Positioning Mechanism," *IEEE Trans. on Industrial Electronics*, Vol. 53, No. 3, pp. 905-914, (2006).

[24] Y. Stepanenko, and C. Su, "Intelligent Control of Piezoelectric Actuators," *Proc. 37th IEEE Conf. Decision and Control*, Tampa, FL, December 1998, pp. 4234-4239.

[25] B. Vautier, and S. Moheimani, "Charge Driven Piezoelectric Actuators for Structural Vibrational Control: Issues and Implementation," *Journal of Smart Materials and Structures*, Vol. 14, pp. 575-586, (2005).

[26] R. Wai, and J. Lee, "Intelligent Motion Control for Linear Piezoelectric Ceramic Motor Drive," *IEEE Trans. on Systems, Man, and Cybernetics - Part B: Cybernetics*, Vol. 34, No. 5, pp. 2100-2111, (2004).

[27] Y. Wu, and Q. Zou, "Iterative Control Approach to Compensate for the Hysteresis and the Vibrational Dynamics Effects of Piezo Actuators," *Proc. IEEE American Control Conference*, Minneapolis, MN, June 2006, 424-429.

[28] Y. Yee, H. Nam, S. Lee, J. Bu, Y. Jeon, and S. Cho, "PZT Actuated Micromirror for Nano-Tracking of Laser Beam for High-Density Optical Data Storage," *Proc. 30th Annual IEEE International Conference on Micro Electro Mechanical Systems (MEMS)*, Jan.2000, pp. 435 - 440.

[29] T. Yeh, S. Lu, and T. Wu, "Modeling and Identification of Hysteresis in Piezoelectric Actuators," *ASME Journal of Dynamic Systems, Measurement, and Control*, Vol. 128, pp. 189-196, (2006).

[30] Y. Xu, and P. Meckl, "Time-Optimal Motion Control of Piezoelectric Actuator: STM Application," *Proc. American Control Conference*, Boston, MA, 2004, pp. 4849-4854.